

University of Nebraska - Lincoln  
**DigitalCommons@University of Nebraska - Lincoln**

---

Stephen Ducharme Publications

Research Papers in Physics and Astronomy

---

2014

# Coplanar switching of polarization in thin films of vinylidene fluoride oligomers

Pankaj Sharma

*University of Nebraska - Lincoln*, [psharma@huskers.unl.edu](mailto:psharma@huskers.unl.edu)

Alexandra Fursina

*University of Nebraska - Lincoln*

Shashi Poddar

*University of Nebraska - Lincoln*


Stephen Ducharme

*University of Nebraska*, [sducharme1@unl.edu](mailto:sducharme1@unl.edu)

Alexei Gruverman

*University of Nebraska-Lincoln*, [agruverman2@unl.edu](mailto:agruverman2@unl.edu)

Follow this and additional works at: <http://digitalcommons.unl.edu/physicsducharme>

 Part of the [Atomic, Molecular and Optical Physics Commons](#), and the [Condensed Matter Physics Commons](#)

---

Sharma, Pankaj; Fursina, Alexandra; Poddar, Shashi; Ducharme, Stephen; and Gruverman, Alexei, "Coplanar switching of polarization in thin films of vinylidene fluoride oligomers" (2014). *Stephen Ducharme Publications*. 101.

<http://digitalcommons.unl.edu/physicsducharme/101>

This Article is brought to you for free and open access by the Research Papers in Physics and Astronomy at DigitalCommons@University of Nebraska - Lincoln. It has been accepted for inclusion in Stephen Ducharme Publications by an authorized administrator of DigitalCommons@University of Nebraska - Lincoln.

# Coplanar switching of polarization in thin films of vinylidene fluoride oligomers

Pankaj Sharma,<sup>a)</sup> Alexandra Fursina,<sup>b)</sup> Shashi Poddar, Stephen Ducharme, and Alexei Gruverman<sup>c)</sup>

Department of Physics and Astronomy and Nebraska Center for Materials and Nanoscience, University of Nebraska, Lincoln, Nebraska 68588, USA

(Received 10 August 2014; accepted 26 October 2014; published online 5 November 2014)

Switching characteristics of vinylidene fluoride oligomer thin films with molecular chains aligned normal to the substrate and exhibiting a preferential in-plane polarization have been investigated using coplanar geometry of inter-digital electrodes via high-resolution piezoresponse force microscopy. It has been shown that in-plane switching proceeds via non-180° rotation of dipoles mediated by non-stochastic nucleation, expansion, and coalescence of domains. As-grown multidomain configuration is found to be strongly pinned aided by charged domain walls, and the electrically induced (in-plane) mono-domain states relax to the as-grown state. The observed coercive field (approximately 0.6 MV/m) is two to three orders of magnitude smaller than that for the oligomer films with out-of-plane polarization. It is suggested that the low steric hindrance to the rotation of molecular dipoles gives rise to the observed low coercive field.

© 2014 AIP Publishing LLC. [<http://dx.doi.org/10.1063/1.4901257>]

Significant research efforts have been put into the discovery and synthesis of new organic/molecular ferroelectrics with the room-temperature polarization comparable to that in oxide ferroelectrics.<sup>1–3</sup> Recent reports feature such materials as donor-acceptor charge transfer complexes,<sup>4,5</sup> supramolecular-assemblies,<sup>6</sup> polar structures with relatively high melting temperature,<sup>2,7</sup> metal-organic coordination compounds,<sup>8,9</sup> and biological tissues.<sup>10,11</sup> These research efforts are focused on uncovering the fundamental mechanisms of molecular ferroelectricity and phase transformations, as well as on designing novel ferroelectric materials for application in electronic devices. Vinylidene fluoride (VDF) based ferroelectrics and their trifluoroethylene (TrFE) copolymers are the most widely studied organic ferroelectrics and used, primarily because of their relatively high polarization value (approximately 10  $\mu\text{C}/\text{cm}^2$ ), biocompatibility, non-toxicity, and ease of large scale fabrication by low cost solvent-based methods. However, a large coercive field (of the order of magnitude 50 MV/m),<sup>12</sup> and consequently, a high operational voltage, is one of the limiting factors in their applications based on polarization reversal. Development of the deposition methods, such as Langmuir-Blodgett (LB)<sup>13</sup> and vacuum evaporation of VDF-oligomers,<sup>14</sup> allowed fabrication of ultra-thin (a few nanometers) films with electrical switchability in the range of several volts. Decreasing the thicknesses below 100 nm, however, results in coercive fields greatly exceeding 50 MV/m, and degradation of ferroelectric properties mainly due to poor crystallinity.<sup>15</sup>

It is well known that the functional properties of molecular materials are strongly dependent on the orientation and conformation of the molecules.<sup>16,17</sup> VDF-oligomers, which

contain a finite number of the VDF units, represent an ideal opportunity to investigate their ferroelectric properties as a function of molecular arrangements controlled by fabrication conditions.<sup>18,19</sup> Previously, VDF-oligomer films with molecular chains aligned parallel to the substrate have been extensively characterized by macroscopic electrical,<sup>20–22</sup> structural,<sup>18,23,24</sup> and local probe-based methods.<sup>14,23,25</sup> In this article, using high-resolution piezoresponse force microscopy (PFM), we have investigated the switching characteristics of the highly crystalline VDF-oligomer thin films with molecular chains oriented normal to the substrate. Several key observations have been made: (i) reversible and reproducible switching of the in-plane polarization occurring via non-180° rotation of dipoles, mediated by deterministic nucleation, expansion, and coalescence of domains; (ii) relaxation of the electrically induced states to the strongly pinned as-grown state; and (iii) an extremely low value of a coercive field in comparison with poly-VDF (PVDF) and its copolymers.

Coplanar rectangular inter-digital electrodes have been used to induce the in-plane polarization reversal in the VDF films. The Ti(2 nm)/Au(20 nm) coplanar inter-digital electrodes were fabricated by electron beam lithography on top of the n-doped Si wafer with 200-nm-thick SiO<sub>2</sub> overlayer (Fig. 1(a)). The spacing between the electrode fingers varied in the range from 2  $\mu\text{m}$  to 8  $\mu\text{m}$  (Fig. 1(b)). After patterning of the electrodes, 20-nm-thick crystalline films of VDF oligomers ( $\text{CF}_3\text{-(CH}_2\text{-CF}_2)_n\text{-I}$ , where  $n = 17 \pm 2$ ) were fabricated using a horizontal Schaefer variation of the LB transfer technique.<sup>26</sup> The oligomer powder was dissolved in dimethylsulfoxide (DMSO) to a concentration of 0.05% by weight and dispersed on the LB trough, compressed to a surface pressure of 5 mN/m and transferred by horizontal contact one layer (monolayer-ML) at a time to the patterned highly doped silicon substrate. The average thickness of a nominal ML, i.e., a layer obtained during a single transfer cycle, is about 4.4 nm.<sup>27</sup> The measured thickness of a 5 ML VDF film is approximately

<sup>a)</sup>psharma@huskers.unl.edu

<sup>b)</sup>Present address: Department of Quantum Nanoscience, Delft University of Technology, P.O. Box 5046, 2600 GA Delft, The Netherlands.

<sup>c)</sup>alexei\_gruverman@unl.edu

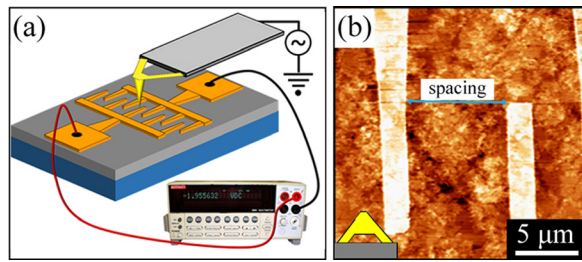


FIG. 1. (a) Schematic illustration of the coplanar switching geometry used to apply planar electric fields. A probing tip under an ac bias is used to visualize in-plane domains in the Lateral PFM mode. (b) AFM topographic image of the VDF oligomer film with a pair of coplanar Au electrodes. Cantilever orientation is shown in image (b).

20 nm determined from the cross-sectional analysis of the topographic AFM images and is well within the oligomer chain length dispersion (i.e.,  $\Delta n = \pm 2$ ). Details of the LB deposition process are similar to that reported in Ref. 27. No subsequent treatment was applied to the samples after the LB deposition process. For macroscopic current-voltage (I-V) investigation, coplanar Al electrodes (length approximately 2 cm, thickness = 100 nm, and spacing approximately 150  $\mu\text{m}$ ) were deposited on the (Si/SiO<sub>2</sub>) doped Si substrate by thermal evaporation, and measurements were performed subsequently after fabrication of a 30 ML VDF film. A commercial atomic force microscope (Asylum MFP-3D) was used in this study to visualize the ferroelectric domain structure. Resonance-enhanced PFM imaging (ac bias: 1 V, frequency range: 200–500 kHz) has been used to visualize the polarization state in the inter-electrode gap (Fig. 1(a)). Conductive triangular Cr/Au-coated ( $k = 0.09 \text{ N/m}$ ) cantilevers have been used in these studies.

Previously,<sup>19,27</sup> it has been established that the molecular chains in the VDF oligomer films fabricated by LB deposition are aligned (nearly) normal to the substrate, with the spontaneous polarization predominantly in the plane of the film. Therefore, to investigate switching characteristics of thin films of VDF-oligomers, coplanar inter-digital electrodes have been employed (Fig. 1(a)). Coplanar electrode geometry allows application of a uniform in-plane switching electric field, while PFM imaging can be performed on the bare VDF surface in the inter-electrode gap (Fig. 1(b)) to monitor evolution of the nucleated domains either in the remanent (the switching field is off during PFM imaging) or in the dynamic, or *in situ*, regime (the switching field is on during PFM imaging). Switching of the remanent in-plane polarization by the  $\pm 5 \text{ V}$ , 1 s electric field pulses has been observed by means of lateral PFM (LPPM) (Figs. 2(a)–2(c)). Importantly, vertical PFM (VPPM) maps (Figs. 2(d)–2(f)) characterized by a low amplitude signal remain mostly unaffected by external field application. As reported earlier,<sup>27</sup> the likely origin of the vertical response signal is a slight inclination of  $-C-C-$  chains away from the substrate normal. In addition, it has been observed that the fully switched in-plane polarization states (supplementary material, Fig. S1)<sup>28</sup> relax over a period of time ranging from several seconds to several minutes. This process manifests itself during repetitive imaging process as appearance of a number of domains of opposite polarity, which gradually grow in size (supplementary material, Fig. S1).

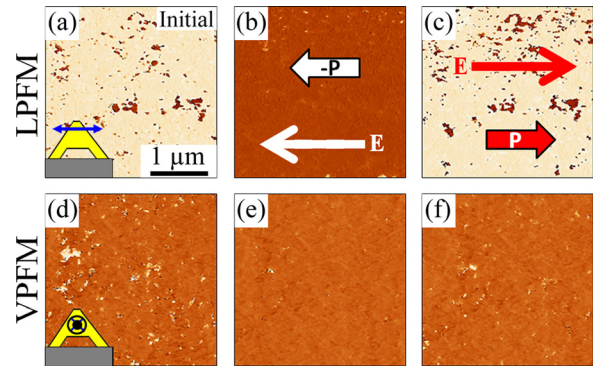


FIG. 2. PFM imaging of the remanent state after in-plane polarization switching. (a)–(c) LPPM phase and (d)–(f) VPPM phase images: (a) and (d) initial state; (b) and (e) after application of the (+5 V, 1 s) pulse; and (c) and (f) after application of the (−5 V, 1 s) pulse. Cantilever orientation is shown in images (a) and (d) with blue arrow on top illustrate cantilever's torsion, whereas a circle with dot indicates vertical deflection. In images (b) and (c), direction of the applied field and in-plane polarization has been indicated. All images are acquired right after application of the switching bias in the remanent state.

To visualize the transition between two opposite in-plane polarization states and to elucidate the mechanism of polarization reversal, *in-situ* PFM imaging with an incrementally changing dc bias has been performed. As can be seen in Figure 3, the switching proceeds via nucleation and growth of irregular domains rather than via the forward growth of high aspect ratio needle-shaped domains along the direction of the applied field as in the case of single crystals. Figure 3 shows the evolution of the x-component of the in-plane polarization, i.e., component along the direction of the applied electric field. To obtain an additional insight into the in-plane polarization reversal, evolution of the y-component of the in-plane polarization (perpendicular to the direction of the applied field) has been studied by the vector-PFM approach.<sup>29</sup> As can be seen in Fig. 4, under a small *in-situ* DC bias ( $\pm 0.5 \text{ V}$ ), the x-component remains mostly unperturbed (Figs. 4(a)–4(c)), while the y-component reverses its direction under a much smaller DC bias ( $\pm 0.2 \text{ V}$ ) (Figs. 4(d)–4(f)). Further increase of a DC bias (until x-component flips too) has no further effect on the y-component. Therefore, the obtained *in-situ* PFM maps (Figs. 3 and 4) point out to a switching process, which proceeds via non-180° rotation of dipoles around  $-C-C-$  molecular chain axis. Specifically, at a smaller field,

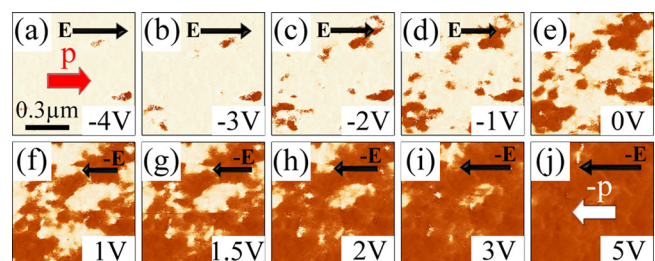


FIG. 3. *In-situ* PFM imaging. (a)–(j) LPPM phase images acquired at an *in-situ* DC bias of −4 V (a), −3 V (b), −2 V (c), −1 V (d), 0 V (e), +1 V (f), +1.5 V (g), +2 V (h), +3 V (i), and +5 V (j), respectively. For images (a)–(d), direction of the applied *in-situ* electric field is to the right, whereas for images (f)–(j), it is to the left. In these images, the detected component of in-plane polarization (i.e., x-component) is along the direction of the applied field.

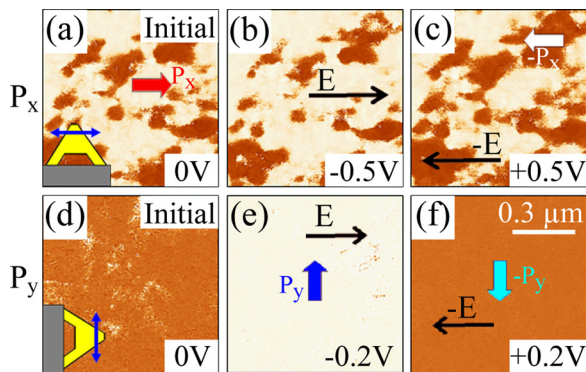


FIG. 4. *In-situ* vector PFM mapping. (a)–(c) LPFM phase images of the component (x) of in-plane polarization along the direction of applied field initially (a), at an *in-situ* DC bias of  $-0.5\text{ V}$  (b), and at an *in-situ* DC bias of  $+0.5\text{ V}$  (c), respectively. (d)–(f) Corresponding LPFM phase images of the component (y) of in-plane polarization perpendicular to the direction of applied field initially (d), at an *in-situ* DC bias of  $-0.2\text{ V}$  (e), and at an *in-situ* DC bias of  $+0.2\text{ V}$  (f), respectively. Cantilever orientation is shown in images (a) and (d). Direction of the applied field and in-plane polarization components have been indicated in the respective images. Images (d)–(f) have been obtained after  $90^\circ$  rotation of the sample.

the in-plane polarization vector toggles by a small angle ( $\theta$ ) which in PFM appears as a reversal of the y-component in combination with the unperturbed x-component. At the stronger external field, the x-component reverses too, which can be interpreted as the in-plane polarization vector rotation by a larger ( $>90^\circ$ ) angle “ $\phi$ ” (supplementary material, Fig. S2).<sup>28</sup> Based on crystal symmetry, polarization reversal in PVDF-based ferroelectrics may progress through successive  $60^\circ$  rotations of molecular dipoles.<sup>30</sup> Thus, it can be argued that at the smaller field, net in-plane polarization vector rotates likely by steps of  $\theta = 60^\circ$  or by  $\phi = 120^\circ$  at higher fields. We also note that the as-grown multidomain (x-component) in-plane polarization state (Fig. 3(e)) was found to be strongly pinned (supplementary material, Fig. S3),<sup>28</sup> and the electrically induced single-domain states always relax to the as-grown state after poling. Moreover, there is a distinct difference between the strongly imprinted as-grown state for the x- and y-components of the in-plane polarization, i.e., a pinned multidomain state for the x-component (Fig. 4(a)) and a nearly single-domain imprinted state for the y-component (Fig. 4(d)).

Figures 3 and 4 also allow an estimate of the coercive field ( $E_c$ ) value. The obtained value of  $E_c$  of about  $0.6\text{ MV/m}$  (supplementary material, Sec. IV)<sup>28</sup> is two to three orders of magnitude lower than the previously reported values for VDF oligomers ( $100\text{--}200\text{ MV/m}$ ),<sup>21</sup> and at least an order of magnitude lower than the lowest coercive field reported for the PVDF-TrFE nanostructures (of order  $10\text{ MV/m}$ ).<sup>31</sup> The coercive field value obtained from analysis of the PFM images is in good agreement with the macroscopic current-voltage measurements (Fig. 5) performed in the LB deposited VDF oligomer films. From the positions of the two switching-current peaks (Fig. 5), the estimated value of coercive field is  $0.23\text{ MV/m}$ . Furthermore, repetitive *in-situ* PFM imaging (Figs. 3 and 4) revealed that the domain nucleation process is deterministic—it always occurs at the same fixed locations. Most of these nucleation sites are located at the grain boundaries (see the inset in Fig. 5).

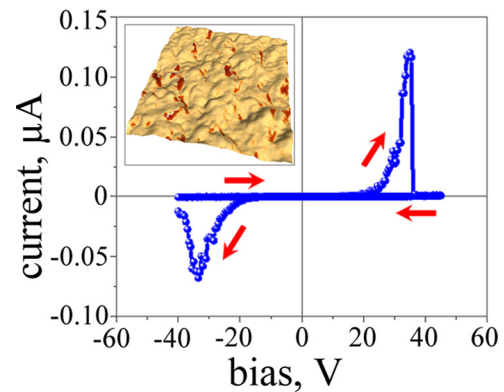


FIG. 5. Polarization switching current obtained using macroscopic Al coplanar electrodes (length  $2\text{ cm}$ , thickness  $100\text{ nm}$ , and spacing  $150\text{ }\mu\text{m}$ ) for a  $30\text{ ML}$  thick VDF oligomer film. Inset—LPFM phase image showing nucleation sites overlaid on the corresponding topographic image.

To shed light on the in-plane switching characteristics of the VDF-oligomer thin films, below we discuss two issues: (i) reasons behind a low coercive field of about  $0.6\text{ MV/m}$  and (ii) causes of the observed domain relaxation in these films. With regard to the first issue, it is worth noting that all the prior investigations were performed in VDF-based ferroelectrics with molecular chains aligned parallel to the substrate. In our case, molecular chains are oriented nearly normal to the substrate and thus each molecular chain has a smaller interaction cross-sectional area at the interface (substrate) than the in-plane oriented molecular chains. This provides a relatively large degree of freedom for the dipole rotation (less steric hindrance<sup>21</sup>) resulting in the low coercive field value.

As far the relaxation is concerned, the initial multidomain in-plane polarization state implies the existence of charged domain walls. For charged domain walls to exist, the bound charges in the bulk associated with discontinuity of polarization should be effectively screened by the mobile charges and/or immobile charged defects. Recent observations<sup>27,32</sup> suggest the existence of stable as-grown charged (head-to-head and tail-to-tail) domain wall configurations in organic ferroelectrics with origin of compensating screening charges yet to be understood. In our case, application of an external (coplanar) electric field removes the charged domain walls; however, the compensating charges (in the bulk) still reside at the same locations as before usually at the grain boundaries (see the inset in Fig. 5), and therefore produce large internal fields,<sup>32</sup> triggering the relaxation of the electrically induced single-domain-states back to the as-grown domain state. Moreover, the observed relaxation is likely aided by incomplete screening of polarization at the coplanar metal electrodes because of poorly defined metal/ferroelectric interface and non-uniform film coverage.

The defining characteristic of the ferroelectric materials is the presence of stable polarization in the absence of an external field. However, the observed relaxation of the electrically induced mono-domain states in these thin films forbids their use in devices relying on hysteretic and stable character of polarization despite a low voltage needed for the polarization reorientation. Here, we suggest a few pathways to address the issue of polarization retention and are as

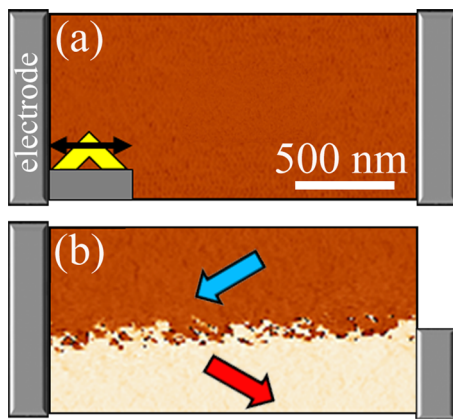


FIG. 6. Planar domain wall. (a) and (b) LPFM phase images detecting  $x$ -component of in-plane polarization: initially (a), and after application of bias with special geometry of electrodes (b). In image (b), possible direction of net in-plane polarization vector has been indicated with schematic illustration of electrodes (in gray color) on the left and right side of the images. These images were acquired in the remanent state.

follows. (1) enhancement of crystallinity to reduce the density of the pinning centers by annealing the samples at temperatures just below the melting point ( $\sim 120$ – $140$  °C); (2) application of strong electric fields for extended periods of time to induce migration and redistribution of the pinned charges; and (3) combination of approaches 1 and 2. In fact, preliminary data (Figure S4) obtained using approach (2) indicate that the polarization retention can be improved by poling the films by strong electric fields.

It should be noted that not all of the domain patterns were unstable. We found that the coplanar inter-digital electrodes allow formation of plane domain walls (Fig. 6). Since the PFM maps in Fig. 4 show a strongly imprinted uniform  $y$ -component, it can be concluded that this wall (likely a  $120^\circ$  domain wall) is electrically neutral. However, strong pinning of the  $x$ -component implies that the charged plane domain walls can be also fabricated using a specific direction of the planar electric field.

In summary, high-resolution PFM has been used to investigate the switching behavior of the VDF-oligomer thin films with a preferential in-plane polarization using a planar geometry of electrodes. Switching of in-plane polarization has been shown to proceed via non- $180^\circ$  rotation of dipoles mediated by deterministic nucleation, expansion, and coalescence of domains. As-grown domain configurations are found to be strongly pinned and characterized by a presence of charged domain walls, which results in the relaxation of the electrically induced states. An unprecedentedly low value of coercive field (0.6 MV/m) is attributed to low steric hindrance to the rotation of molecular dipoles in the molecular chains aligned normal to the substrate. The obtained results may spur further studies of the switching dynamics and electronic properties of the planar domain walls in ferroelectric polymer films.

This research was supported by the U.S. Department of Energy, Office of Basic Energy Sciences, Division of Materials Sciences and Engineering under Award No. DE-

SC0004530 (switching characterization), by the National Science Foundation under Grants MRSEC DMR-0820521 and ECCS-1101256 (electrode fabrication), and by the Nebraska EPSCoR Trans-disciplinary, Multi-Institutional Research Clusters Program (VDF films fabrication).

- <sup>1</sup>S. Horiuchi and Y. Tokura, *Nat. Mater.* **7**, 357 (2008).
- <sup>2</sup>D.-W. Fu, H.-L. Cai, Y. Liu, Q. Ye, W. Zhang, Y. Zhang, X.-Y. Chen, G. Giovannetti, M. Capone, J. Li, and R.-G. Xiong, *Science* **339**, 425 (2013).
- <sup>3</sup>J. Li, Y. Liu, Y. Zhang, H.-L. Cai, and R.-G. Xiong, *Phys. Chem. Chem. Phys.* **15**, 20786 (2013).
- <sup>4</sup>E. Collet, M. H. Lemee-Cailleau, M. Buron-Le Cointe, H. Cailleau, M. Wulff, T. Luty, S. Y. Koshihara, M. Meyer, L. Toupet, P. Rabiller, and S. Techert, *Science* **300**, 612 (2003).
- <sup>5</sup>A. S. Tayi, A. K. Shveyd, A. C. H. Sue, J. M. Szarko, B. S. Rolczynski, D. Cao, T. J. Kennedy, A. A. Sarjeant, C. L. Stern, W. F. Paxton, W. Wu, S. K. Dey, A. C. Fahrenbach, J. R. Guest, H. Mohseni, L. X. Chen, K. L. Wang, J. F. Stoddart, and S. I. Stupp, *Nature* **488**, 485 (2012).
- <sup>6</sup>S. Horiuchi, F. Ishii, R. Kumai, Y. Okimoto, H. Tachibana, N. Nagaosa, and Y. Tokura, *Nat. Mater.* **4**, 163 (2005).
- <sup>7</sup>D. W. Fu, W. Zhang, H. L. Cai, J. Z. Ge, Y. Zhang, and R. G. Xiong, *Adv. Mater.* **23**, 5658 (2011).
- <sup>8</sup>B. Kundys, A. Lappas, M. Viret, V. Kapustianyk, V. Rudyk, S. Semak, C. Simon, and I. Bakaimi, *Phys. Rev. B* **81**, 224434 (2010).
- <sup>9</sup>W. Zhang and R. G. Xiong, *Chem. Rev.* **112**, 1163 (2012).
- <sup>10</sup>Y. Liu, Y. Zhang, M.-J. Chow, Q. N. Chen, and J. Li, *Phys. Rev. Lett.* **108**, 078103 (2012).
- <sup>11</sup>D. Denning, M. T. Abu-Rub, D. I. Zeugolis, S. Habelitz, A. Pandit, A. Fertala, and B. J. Rodriguez, *Acta Biomater.* **8**, 3073 (2012).
- <sup>12</sup>T. Furukawa, *Phase Transitions* **18**, 143 (1989).
- <sup>13</sup>S. Palto, L. Blinov, A. Bune, E. Dubovik, V. Fridkin, N. Petukhova, K. Verkhovskaya, and S. Yudin, *Ferroelectr., Lett.* **19**, 65 (1995).
- <sup>14</sup>K. Noda, K. Ishida, A. Kubono, T. Horiuchi, H. Yamada, and K. Matsushige, *Jpn. J. Appl. Phys., Part 1* **39**, 6358 (2000).
- <sup>15</sup>V. Fridkin and S. Ducharme, *Ferroelectricity at the Nanoscale* (Springer-Verlag, Berlin, 2014), p. 43.
- <sup>16</sup>G. Qian, S. Saha, and K. M. Lewis, *Appl. Phys. Lett.* **96**, 243107 (2010).
- <sup>17</sup>M. C. Petty, M. R. Bryce, and D. Bloor, *Introduction to Molecular Electronics* (Oxford University Press, New York, 1995).
- <sup>18</sup>S. Kuwajima, S. Horie, T. Horiuchi, H. Yamada, K. Matsushige, and K. Ishida, *Macromolecules* **42**, 3353 (2009).
- <sup>19</sup>R. Korlacki, J. T. Johnson, J. Kim, S. Ducharme, D. W. Thompson, V. M. Fridkin, Z. Ge, and J. M. Takacs, *J. Chem. Phys.* **129**, 064704 (2008).
- <sup>20</sup>K. Noda, K. Ishida, T. Horiuchi, H. Yamada, and K. Matsushige, *Jpn. J. Appl. Phys., Part 2* **42**, L1334 (2003).
- <sup>21</sup>K. Noda, K. Ishida, A. Kubono, T. Horiuchi, H. Yamada, and K. Matsushige, *J. Appl. Phys.* **93**, 2866 (2003).
- <sup>22</sup>S. Chen, K. Yao, and F. E. H. Tay, *Polym. Int.* **61**, 169 (2012).
- <sup>23</sup>K. Noda, K. Ishida, T. Horiuchi, K. Matsushige, and A. Kubono, *J. Appl. Phys.* **86**, 3688 (1999).
- <sup>24</sup>Y. Kuroda, Y. Koshihara, M. Misaki, S. Horie, K. Ishida, and Y. Ueda, *Jpn. J. Appl. Phys., Part 1* **51**, 04DK05 (2012).
- <sup>25</sup>K. Matsushige and H. Yamada, *Ann. N. Y. Acad. Sci.* **960**, 1 (2002).
- <sup>26</sup>S. Ducharme, S. P. Palto, and V. M. Fridkin, in *Handbook of Thin Film Materials*, edited by H. S. Nalwa (Academic Press, San Diego, 2002), Vol. 3.
- <sup>27</sup>P. Sharma, S. Poddar, R. Korlacki, S. Ducharme, and A. Gruverman, *Appl. Phys. Lett.* **105**, 022906 (2014).
- <sup>28</sup>See supplementary material at <http://dx.doi.org/10.1063/1.4901257> for experimental details on polarization relaxation, switching of in-plane polarization, pinned as-grown state, estimation of coercive field, and polarization retention.
- <sup>29</sup>S. V. Kalinin, B. J. Rodriguez, S. Jesse, J. Shin, A. P. Baddorf, P. Gupta, H. Jain, D. B. Williams, and A. Gruverman, *Microsc. Microanal.* **12**, 206 (2006).
- <sup>30</sup>T. Furukawa, T. Nakajima, and Y. Takahashi, *IEEE Trans. Dielectr. Electr. Insul.* **13**, 1120 (2006).
- <sup>31</sup>Z. Hu, M. Tian, B. Nysten, and A. M. Jonas, *Nat. Mater.* **8**, 62 (2009).
- <sup>32</sup>F. Kagawa, S. Horiuchi, N. Minami, S. Ishibashi, K. Kobayashi, R. Kumai, Y. Murakami, and Y. Tokura, *Nano Lett.* **14**, 239 (2014).